Accepted for publication in ApJ on 22 Aug 2016
Preprint typeset using LaTeX style emulateapj v. 5/2/11

arXiv:1608.06283v2 [astro-ph.GA] 30 Sep 2016

880 μm SMA POLARIZATION OBSERVATIONS OF THE QUASAR 3C 286

Charles L. H. Hull[1,2], Josep M. Girart[1,3], and Qizhou Zhang[1]

Accepted for publication in ApJ on 22 Aug 2016

ABSTRACT

For decades the bright radio quasar 3C 286 has been widely recognized as one of the most reliable polarization calibrators at centimeter wavelengths because of its unchanging polarization position angle and high polarization percentage. However, it has become clear in recent years that the polarization position angle of 3C 286 changes with increasing frequency, increasing from $\sim 33^\circ$ at $\lambda \gtrsim 3$ cm to $\sim 38^\circ$ at $\lambda \approx 1$ mm. With the advent of high-sensitivity polarization observations by current and future (sub)millimeter telescopes, knowledge of the position angle of 3C 286 at higher frequencies is critical for calibration. We report the first polarization observations of 3C 286 at submillimeter wavelengths, taken at 880 μm (340 GHz) with the Submillimeter Array. We find a polarization position angle and percentage of $37.4 \pm 1.5^\circ$ and $15.7 \pm 0.8\%$, respectively, consistent with previous measurements at 1 mm.

Subject headings: polarization — quasars: individual (3C 286) — instrumentation: polarimeters — techniques: polarimetric — techniques: interferometric — methods: observational

1. INTRODUCTION

3C 286 is a bright, highly polarized quasar at a redshift $z = 0.849$ (Burbidge & Burbidge 1969) with exceptionally stable polarization properties. For decades 3C 286 has been known to have an unchanging polarization position angle of 33° (measured counter-clockwise, or east, from north) and a polarization percentage of $\sim 10\%$ at radio wavelengths ($\sim$1.4–6 GHz; Perley 1982), making it an ideal calibrator for radio telescopes in the northern hemisphere such as the Very Large Array (now the Karl G. Jansky Very Large Array; VLA) and the Very Long Baseline Array (VLBA). Perley & Butler (2013) performed dedicated VLA observations of 3C 286 and other calibrators from $\sim$1–44 GHz, again confirming the robustness of 3C 286 as a polarization calibrator at $\nu \lesssim 6$ GHz. However, Perley & Butler note that the position angle of 3C 286 appears to increase slowly as a function of frequency above ~ 9 GHz, reaching an angle of 36° at 43.5 GHz. Higher frequency polarization observations of 3C 286 are critical if it is to be used as an absolute polarization calibrator at short wavelengths.

There have been several observations of 3C 286 at 3 mm and 1 mm that confirm this increase in polarization angle, including work by Marrone (2006); Agudo et al. (2012); Hull & Plambeck (2015); Nagai et al. (2016),[4] finding position angles of $\sim$36–41°, consistent with the increase seen by Perley & Butler (2013). Here we report the first submillimeter polarization observations of 3C 286, taken at 880μm (340 GHz) with the Submillimeter Array (SMA; Ho et al. 2004).[5] We find a polarization position angle and percentage of $37.4 \pm 1.5^\circ$ and $15.7 \pm 0.8\%$, respectively, consistent with previous measurements at 1 mm, suggesting that the polarization angle plateaus at $\sim 38^\circ$ at high frequencies.

2. OBSERVATIONS AND CALIBRATION

We performed 880μm SMA continuum polarization observations of 3C 286 (α_{J2000} = 13:31:08.2879, δ_{J2000} = +30:30:32.958) as a filler track (2015B-S068; PI: Charles L. H. Hull) on 2016 January 28 in the compact configuration, with a resolution of $\sim 1\farcs8$.

The observations were made using the SMA polarization receiver system (Marrone 2006; Marrone & Rao 2008) in dual-receiver, full-polarization mode. The lower sideband (LSB) and upper sideband (USB) of each receiver had 2 GHz of bandwidth, ranging from 334.126–336.004 GHz (LSB) and 344.126–346.004 GHz (USB).[6] The average (band-center) frequencies of the two sidebands are 335.065 GHz (LSB) and 345.056 GHz (USB), corresponding to approximately 895 and 870 μm, respectively.

Unlike in single-receiver mode where wave-plate switching is required to measure all four cross correlations (RR, LL, LR, RL) between the left- (L) and right- (R) circularly polarized signals, in dual-receiver mode all correlations are measured simultaneously, with the 300 GHz receiver measuring L and the 400 GHz receiver measuring R when the quarter-wave plates are in the "left" position. The quarter-wave plates on antennas 1 and 4 were periodically switched to the "right" position during observations

chat.hull@cfa.harvard.edu
[1] Harvard-Smithsonian Center for Astrophysics, 60 Garden St., Cambridge, MA 02138, USA
[2] Jansky Fellow of the National Radio Astronomy Observatory
[3] Institut de Ciències de l'Espai, (CSIC-IEEC), Campus UAB, Carrer de Can Magrans S/N, 08193 Cerdanyola del Vallès, Catalonia, Spain

[4] See also the Atacama Large Millimeter-submillimeter Array (ALMA) CASA Guide on 3C 286 polarization at 1 mm; Nagai et al. (2016) report results from the same 1 mm Science Verification data: `https://casaguides.nrao.edu/index.php/3C286_Polarization`

[5] The Submillimeter Array is a joint project between the Smithsonian Astrophysical Observatory and the Academia Sinica Institute of Astronomy and Astrophysics, and is funded by the Smithsonian Institution and the Academia Sinica.

[6] While the observations we present have a total bandwidth of 4 GHz, the advent of the new SWARM correlator (SMA Wideband Astronomical ROACH2 Machine) will enable future dual-receiver, full-polarization observations with greater bandwidths.

of the bright calibrator 3C 84 in order to calibrate the cross-receiver delay and the *RL*-phase offset between the 300 and 400 GHz receivers; this allowed us to calibrate the absolute position angle of the polarized radiation.

We performed the initial calibration—flagging, bandpass, cross-receiver delays, complex gains, flux calibration, and *RL*-phase offset—using the IDL superset `MIR` (see Qi & Young 2015 for a description of how to calibrate polarization data in `MIR`). Antennas 5 and 7 were out of the array. The weather was excellent, with a 225 GHz zenith opacity $\tau_{225} < 0.04$ for nearly the entire observation. The double-sideband (DSB) system temperatures were between 145 and 216 K.

After initial calibration we exported the data to `MIRIAD` (Sault et al. 1995), which we used for measuring the polarization leakage terms and for imaging. 3C 286 has a flux of $\sim 240\,\mathrm{mJy\,beam^{-1}}$ at 880μm, and was thus too weak to use as a polarization leakage calibrator. Consequently, the 3C 286 observation was performed directly after another full-polarization track (2015B-S012, PI: Laurence Sabin), which included 3C 84, a bright calibrator suitable for polarization calibration. After one round each of amplitude and phase self-calibration on 3C 84, we measured leakage terms and applied them to the 3C 286 data. The leakage terms had amplitudes $< 1.5\%$ for all antennas in both sidebands.

3. RESULTS

We used `MIRIAD` to produce Stokes I, Q, and U continuum images using natural weighting (`robust` $= 2$, also `sup` $= 0$ in `MIRIAD`). The phases of 3C 286 were corrected with one round of phase-only self calibration. The final synthesized beam is $1\farcs89 \times 1\farcs80$ at a position angle of $-19°$, and the rms noise levels in the Stokes I, Q, and U maps are all $\sim 2\,\mathrm{mJy\,beam^{-1}}$.

We find that 3C 286 has a polarization position angle and percentage at 880 μm of $37.4 \pm 1.5°$ and $15.7 \pm 0.8\%$, respectively. These results are consistent with previous measurements at 1 mm. We show the Stokes I total intensity map with polarization orientation overlaid in Figure 1, and the Stokes Q and U maps in Figure 2. Note that measurements of polarized intensity $P = \sqrt{Q^2 + U^2}$ should generally be debiased (Vaillancourt 2006; Hull & Plambeck 2015); however, the signal-to-noise ratio (SNR) of P always exceed ~ 13, and thus the debiased value of the polarized intensity is unchanged to within the uncertainty of the original value.

Previous studies of 3C 286 with the VLA and CARMA (the Combined Array for Research in Millimeter-wave Astronomy) used the polarization of Mars to calibrate the absolute position angle of the telescope (Perley & Butler 2013; Hull & Plambeck 2015), as rocky planets or satellites are expected to have polarization that is radial with respect to the planet's disk (Heiles & Drake 1963; Davies & Gardner 1966; White & Cogdell 1973; Perley & Butler 2013). Unfortunately, this test of absolute position angle has not yet been performed with the SMA dual-receiver polarization system. However, the SMA has the unique advantage of using quarter-wave plates, which have very well known polarization properties (Marrone 2006). Given a high enough SNR of the calibrator used to derive the cross-receiver delay and *RL*-phase offset, the polarization position angle accuracy is limited only by the rotation of the wave plates, which are positioned with an accuracy $\ll 1°$ (Marrone 2006; Marrone et al. 2007).

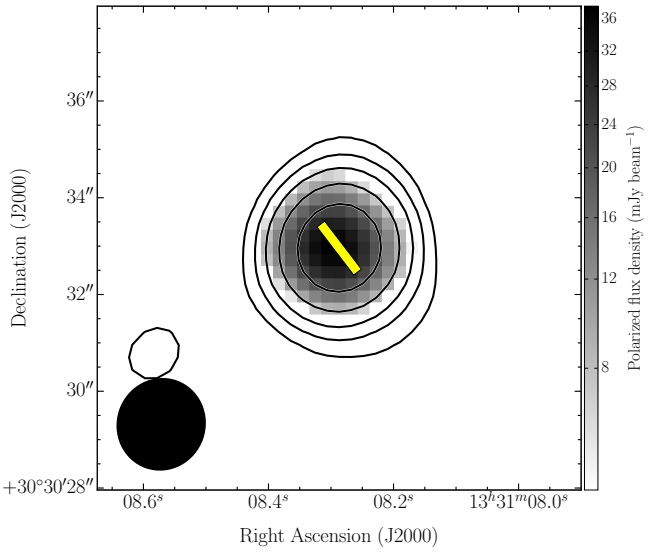

Figure 1. 880 μm SMA image of 3C 286 ($\alpha_{\mathrm{J2000}} = 13{:}31{:}08.2879$, $\delta_{\mathrm{J2000}} = +30{:}30{:}32.958$). The rms noise level in the Stokes I map $\sigma_I = 2\,\mathrm{mJy\,beam^{-1}}$. The black contours are the Stokes I total intensity at $-3, 3, 8, 16, 32, 64 \times \sigma_I$. Grayscale is the polarized flux density $P = \sqrt{Q^2 + U^2}$. The peak polarization percentage P/I is $15.7 \pm 0.8\%$. The yellow line segment is the polarization position angle $\chi = 37.4 \pm 1.5°$. The ellipse in the lower left represents the synthesized beam, which measures $1\farcs89 \times 1\farcs80$ at a position angle of $-19°$.

At (sub)millimeter wavelengths, 3C 286 has a polarization position angle $\chi \approx 38°$, where $\chi = 0.5 \arctan(U/Q)$. Somewhat inconveniently, this value is close to $\chi = 45°$, where, by definition, all of the signal is in Stokes U and none is in Stokes Q. The 38° position angle implies that the Stokes Q signal is 4 times weaker than the Stokes U signal. At a high enough noise level (i.e., a SNR of the polarization emission $\lesssim 8$) the Stokes Q signal would be undetectable, leading us to derive an incorrect position angle $38° < \chi < 45°$. The value would be $< 45°$ because when calculating χ the value for Q would not be identically zero, but would be an upper limit dictated by the rms noise in the Stokes Q map.

Furthermore, the standard CLEAN process on independent Stokes Q and U visibilities fails to properly account for the complex vector nature of the linear polarization when the signal is weak (e.g., Pratley & Johnston-Hollitt 2016). Pratley & Johnston-Hollitt (2016) described a method for `CLEANing` that avoids this bias in low-signal-to-noise polarization observations, particularly in extended sources. Fortunately, the combined (DSB) SMA data we present here are sensitive enough that the Stokes Q map has a SNR $\gtrsim 3\,\sigma_P$, and 3C 286 is a point source at SMA resolution, therefore this type of novel imaging approach is not necessary.

In short, the only results to date with high-SNR Stokes Q maps are the 1 mm ALMA results from Nagai et al. (2016) and the 880 μm SMA results presented here, both of which yield polarization position angles of $\chi \approx 38°$, suggesting that there is no continued increase in the position angle of 3C 286 at $\lambda \lesssim 1\,\mathrm{mm}$ ($\nu \gtrsim 230\,\mathrm{GHz}$).

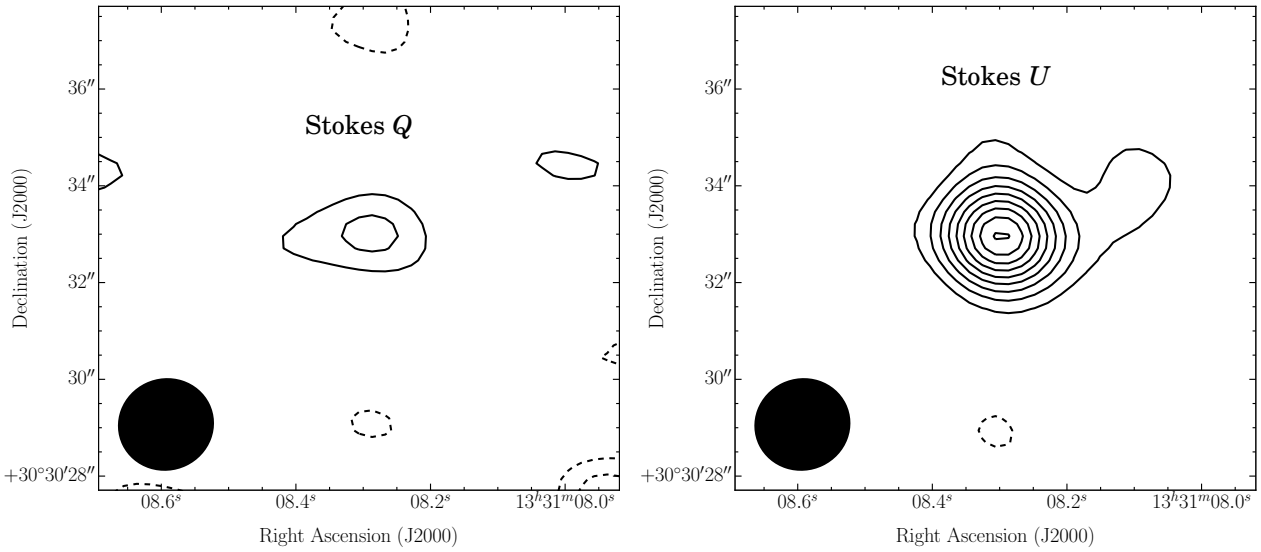

Figure 2. Stokes Q and U maps of 3C 286. The rms noise levels in the Stokes Q, and U maps $\sigma_Q = \sigma_U = \sigma_P = 2\,\mathrm{mJy\,beam^{-1}}$. Black contours are the Stokes Q (left) and U (right) intensities at $-3, -2, 2, 4, 6, 8, 10, 12, 14, 16, 18 \times \sigma_P$. As in Figure 1, the ellipses in the lower left represent the synthesized beam.

4. DISCUSSION AND SUMMARY

In Figure 3 we extend the work of Perley & Butler (2013) and show the polarization angle and percentage of 3C 286 as a function of frequency from $\sim 1 - 340$ GHz, now including the results from the Institut de Radioastronomie Millimétrique (IRAM) 30 m telescope (3 mm, 1 mm: Agudo et al. 2012), CARMA (1 mm: Hull & Plambeck 2015), ALMA (1 mm: Nagai et al. 2016), and the SMA (1 mm: Marrone 2006; 880μm: this work).

Table 1: SMA 880 μm polarization results

I $\left(\frac{\mathrm{mJy}}{\mathrm{beam}}\right)$	Q $\left(\frac{\mathrm{mJy}}{\mathrm{beam}}\right)$	U $\left(\frac{\mathrm{mJy}}{\mathrm{beam}}\right)$	χ (°)	Π (%)
241.7 ± 2.0	10.0 ± 2.0	36.7 ± 2.0	37.4 ± 1.5	15.7 ± 0.8

Table 1
Stokes I, Q, and U fluxes, polarization position angle, and polarization percentage derived from the combined (DSB) 880 μm (340 GHz) SMA data. The uncertainties in the I, Q, and U maps are the rms noise values measured from the maps; the uncertainties in the polarization position angle and percentage are calculated using standard error propagation.

The polarization position angle of 3C 286 appears to be constant at $\sim 33°$ at $\nu \lesssim 8$ GHz, and constant at $\sim 38°$ at $\nu \gtrsim 230$ GHz. The simplest explanation of the change in polarization position angle is a change in the position angle of either the jet or the magnetic field with distance from the nucleus, combined with a gradient in the spectral index of the emission along the jet. In other words, we are most likely probing two different components at low and high frequencies: a population of less energetic electrons downstream in the jet that dominate the centimeter-wave emission, and a more energetic population of electrons further upstream (near the nucleus of the AGN) that dominate the (sub)millimeter-wave emission. The observations at intermediate frequencies (~ 8–230 GHz) where the polarization position angle changes from 33–38° are probing a combination of the two regions.[7]

High-resolution (milliarcsecond-scale) observations of 3C 286 using very long baseline interferometry (VLBI) from ~ 1.6–15 GHz were performed in several studies including Zhang et al. (1994); Akujor & Garrington (1995); Jiang et al. (1996); Cotton et al. (1997); Nagai et al. (2016), all of which report an elongated jet extending ~ 50 mas to the southwest of the nucleus. Akujor & Garrington (1995); Jiang et al. (1996); Cotton et al. (1997) report polarization data, showing that both the nucleus and the SW jet have a polarization position angle that is consistent (on average) with the 33° position angle assumed for 3C 286 at long wavelengths. However, as noted above, the effective weighting of the polarization in the jet and the nucleus will be drastically different at (sub)millimeter frequencies. Further discussion of the change in polarization position angle as a function of frequency can be found in Cotton et al. (1997); Agudo et al. (2012); Nagai et al. (2016).

Because of the difficulty of high-frequency observations and the decreasing flux of 3C 286 at higher frequencies, polarimetric observations of 3C 286 at $\nu > 340$ GHz ($\lambda < 880\mu$m) are impossible (or impractical) with current instruments. To determine whether the position angle remains steady at $\sim 38°$ at $\nu > 340$ GHz will require confirmation by the ALMA Band 8 (440 GHz), 9 (660 GHz), and 10 (870 GHz) polarization systems, which have yet to be commissioned. Characterization of 3C 286 at these high frequencies will soon be essential: as millimeter, submillimeter, and far-infrared telescope sensitivity improves, 3C 286 will continue to be an invaluable calibrator for high-frequency polarization observations.

[7] The "intermediate frequencies" where the polarization position angle of 3C 286 changes could be anywhere from ∼8–86 GHz to ∼ 8–230 GHz, since there are no available polarization observations between the 86 GHz observations from IRAM and the 230 GHz observations from CARMA and ALMA.

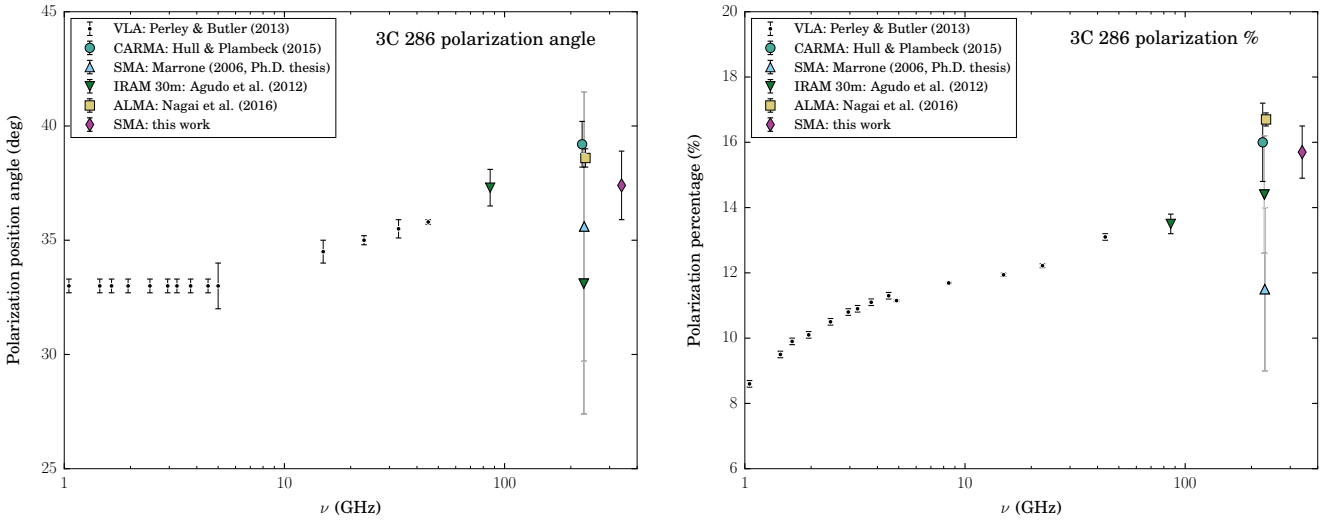
VLA: Perley & Butler (2013)
CARMA: Hull & Plambeck (2015)
SMA: Marrone (2006, Ph.D. thesis)
IRAM 30m: Agudo et al. (2012)
ALMA: Nagai et al. (2016)
SMA: this work
3C 286 polarization angle
Polarization position angle (deg)
ν (GHz)
3C 286 polarization %
Polarization percentage (%)
ν (GHz)

Figure 3. 3C 286 polarization position angle (left) and percentage (right) as a function of frequency. The data can be found in Perley & Butler (2013) (VLA: $\sim$1–45 GHz)†; Agudo et al. (2012) (IRAM 30 m: 3 mm, 1 mm); Hull & Plambeck (2015) (CARMA: 1 mm); Nagai et al. (2016) (ALMA: 1 mm); Marrone (2006) (SMA: 1 mm); and this work (SMA: 880μm). The CARMA polarization percentage was provided by Dick Plambeck (2016, private communication), and is associated with the 04 May 2014 observations listed in Table 3 of Hull & Plambeck (2015). The 1 mm data points from Agudo et al. (2012) and Marrone (2006), which have high uncertainties, have been plotted with light gray error bars to highlight the higher-SNR data.

† Polarization angle and percentage values at $\nu \leq 45$ GHz include those from Table 3 ($\nu < 5$ GHz) and Tables 2 and 5 ($\nu \geq 4.885$ GHz) of Perley & Butler (2013). The Table 3 values have been assigned errors in polarization percentage and angle of $\delta\Pi = 0.1\%$ and $\delta\chi = 0.3°$, where the former is the typical residual polarization percentage in a VLA map of an unpolarized source (Rick Perley, 2016, private communication), and the latter is calculated by standard error propagation: $\delta\chi = 0.5 \arctan(\delta\Pi/\Pi)$. Note that the $\nu > 4.885$ GHz data from Tables 2 and 5 of Perley & Butler 2013 at are not at exactly the same frequency in the two plots. The polarization percentage values at low frequencies have not been corrected for the increase as a function of time reported by Perley & Butler (2013).

The authors thank the anonymous referee for the insightful comments. C.L.H.H. thanks the SMA staff who made the SMA observations possible. He particularly thanks Charlie Qi for his help with `MIR` data reduction. He also thanks Ram Rao and Dan Marrone for the useful discussion of absolute polarization angle calibration of the SMA. C.L.H.H. thanks Laurence Sabin for kindly allowing us to use data from her project 2015B-S012 to measure polarization leakage terms necessary to calibrate the 3C 286 data. C.L.H.H. acknowledges Dick Plambeck for his help in deriving polarization percentages and uncertainties from the 1 mm CARMA data, and Rick Perley for the discussion of the low-frequency data from Perley & Butler (2013). J.M.G. acknowledges support from MICINN AYA2014-57369-C3-P and the MECD PRX15/00435 grants (Spain). Q.Z. and J.M.G. acknowledge the support of the SI CGPS award, "Magnetic Fields and Massive Star Formation." The National Radio Astronomy Observatory is a facility of the National Science Foundation operated under cooperative agreement by Associated Universities, Inc. This research made use of APLpy, an open-source plotting package for Python hosted at `http://aplpy.github.com`.

REFERENCES

Agudo, I., Thum, C., Wiesemeyer, H., et al. 2012, A&A, 541, A111
Akujor, C. E., & Garrington, S. T. 1995, A&AS, 112, 235
Burbidge, G. R., & Burbidge, E. M. 1969, Nature, 222, 735
Cotton, W. D., Fanti, C., Fanti, R., et al. 1997, A&A, 325, 479
Davies, R. D., & Gardner, F. F. 1966, Australian Journal of Physics, 19, 823
Heiles, C. E., & Drake, F. D. 1963, Icarus, 2, 281
Ho, P. T. P., Moran, J. M., & Lo, K. Y. 2004, ApJ, 616, L1
Hull, C. L. H., & Plambeck, R. L. 2015, Journal of Astronomical Instrumentation, 4, 1550005
Jiang, D. R., Dallacasa, D., Schilizzi, R. T., et al. 1996, A&A, 312, 380
Marrone, D. P. 2006, PhD thesis, Harvard University
Marrone, D. P., Moran, J. M., Zhao, J.-H., & Rao, R. 2007, ApJ, 654, L57
Marrone, D. P., & Rao, R. 2008, in Society of Photo-Optical Instrumentation Engineers (SPIE) Conference Series, Vol. 7020, Society of Photo-Optical Instrumentation Engineers (SPIE) Conference Series
Nagai, H., Nakanishi, K., Paladino, R., et al. 2016, ApJ, 824, 132
Perley, R. A. 1982, AJ, 87, 859
Perley, R. A., & Butler, B. J. 2013, ApJS, 206, 16
Pratley, L., & Johnston-Hollitt, M. 2016, MNRAS, 462, 3483
Qi, C., & Young, K. 2015, SMA Technical Memos, 160
Sault, R. J., Teuben, P. J., & Wright, M. C. H. 1995, in ASP Conf. Ser. 77: Astronomical Data Analysis Software and Systems IV, ed. R. A. Shaw, H. E. Payne, & J. J. E. Hayes, Vol. 4, 433
Vaillancourt, J. E. 2006, PASP, 118, 1340
White, T. L., & Cogdell, J. R. 1973, Moon, 6, 235
Zhang, F. J., Spencer, R. E., Schilizzi, R. T., et al. 1994, A&A, 287, 32